Kinetics, isotherms and thermodynamic modelling of reactive blue 52 and reactive orange 107 dyes from aqueous solution using PANI-CoCl$_2$ as adsorbent

U D Lingeswari & T Vimala*

PG & Research Department of Chemistry, Seethalakshmi Ramaswami College (Affiliated to Bharathidasan University),
Tiruchirappalli-620002, Tamil Nadu, India

Email: vimalsrc@gmail.com, udlingeswari@gmail.com

In this work decolourisation of organic dyes such as Reactive Blue 52 and Reactive Orange 107 from aqueous solution by PANI-CoCl$_2$ composite have been studied. Polyaniline (PANI) is a viable conducting polymer because of its unique proton dopability, excellent redox recyclability, chemical stability, variable electrical conductivity, low cost and ease of synthesis. The morphology of PANI-CoCl$_2$ composite have been characterized by scanning electron microscopy and Fourier transform infrared spectroscopy. It is also shown that many factors affected the adsorption rate, such as adsorbent mass, contact time, variation of pH, agitation speed, dye concentration and temperature. The capacity of the adsorbent is tested using recyclability process. Adsorption of Reactive Blue 52 and Reactive Orange 107 by PANI-CoCl$_2$ follows pseudo-second-order kinetics and the best-fit isotherm is the Langmuir model which is confirmed by using correlation coefficients in ANOVA technique. The thermodynamic parameters like changes in free energy, enthalpy and entropy have been also calculated.

A dye is a coloured organic substance or mixture either forms a chemical or physical interaction with the substance being dyed. Dyeing processes are generally carried out using water as the medium. One of the main threatening problems of the industrial world is the pollution of water and the wastewater from dying industries has been found to pollute the neighbouring water resources. Dyes possess a high tendency to affect the natural process like photosynthesis. Reactive dyes are known to cause contact dermatitis[1] and asthma[2]. Some of the important methods widely practiced to treat effluents are biological, physical, chemical and adsorption processes[3-5]. Among these methods, the most promising and cost-effective method is the adsorption process. Adsorption technique is used for the removal of dye from water because it is an efficient, easy to handle and low-cost technique. Researchers have investigated adsorption using carbon-based materials such as coconut coir[6], olive stone[7], orange peel[8], banana pith[9], rice husk[10] and corncob,[11], etc., as adsorbents for the removal of anionic dyes. Processing of natural adsorbent to the required amount at all seasons is difficult and hence the researchers need to probe the alternatives. The emeraldine salt of polyaniline (PANI) has been used successfully for the selective removal of anionic dyes from aqueous solution[12,13]. The interaction between the anion part of sulphoinc acid dye molecule and the positively charged PANI backbone is responsible for the adsorption of anionic dye onto PANI-Composite from aqueous dye solution. In earlier studies, CuCl$_2$ has been used to dope PANI which increases the percentage of removal of dye[14,15]. A perusal of literature revealed that there is no adsorption study reported using PANI-CoCl$_2$ as an adsorbent for the removal of dyes. Hence we have scrutinized the ability of PANI-CoCl$_2$ as an adsorbent to remove anionic single azo [Reactive Orange 107 (RO 107)] and double azo dyes [Reactive Blue 52 (RB52)].

Materials and Methods

Materials

Aniline and HCl were obtained from Merck specialties (P) Ltd., Mumbai. Ammonium persulphate was obtained from Loba chemie Pvt. Ltd., Mumbai. CoCl$_2$ was obtained from Nice chemicals Pvt. Ltd., Kerala. Reactive Blue 52 (RB 52) and Reactive Orange 107 (RO 107) used in the adsorption studies were procured and used as such. The structures of the dyes are shown in Fig. 1a and 1b.

Instruments

In the experimental studies, MAPADA V-1100D spectrophotometer was used for the determination of dye concentrations. Equip-Tronics digital pH meter model EQ-610 was used in pH measurements. R-8C Laboratory centrifuge, REMI motors was used to centrifuge the dye solution. Magnetic stirrer REMI Electro Technik LTD was used to stir the dye solution.

Preparation of PANI-CoCl₂

By chemical oxidation coupled with polymerization, cobalt chloride doped PANI was synthesized with ammonium persulphate as an oxidant. Ammonium persulphate was dissolved in water and mixed with the solution of aniline in acidic medium (1.5 N HCl) and diluted CoCl₂ of required percentage dissolved in water was added to the solution mixture and stirred in magnetic stirrer at 400 rpm for 4 h. The dark green CoCl₂ doped PANI sample was precipitated. On completion of polymerization PANI-CoCl₂ composite from solution was filtered, washed, dried and stored[16, 17]. Structure of PANI-cobalt chloride (PANI-CoCl₂) [16] is shown in Fig. 2.

Standardization of dye solution

The cuvette was filled with dye solution up to the mark and by using MAPADA V-1100D spectrophotometer optical density (OD) was measured.
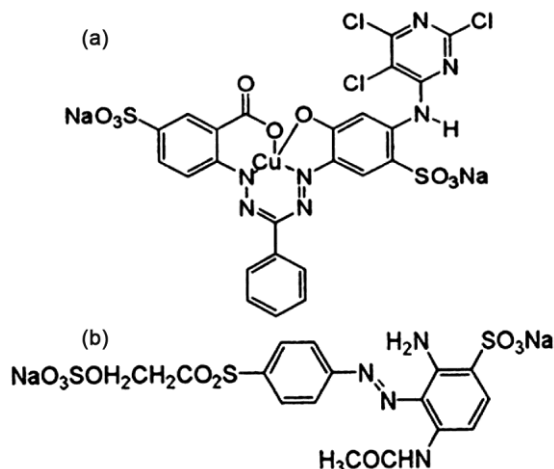

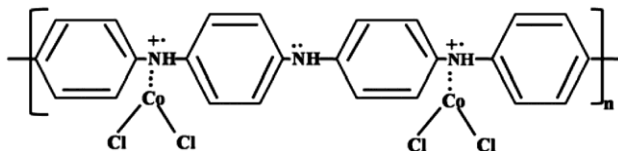Fig. 1 — Structure of (a) RB 52 and (b) RO 107 dye.

Fig. 2 — Structure of PANI-CoCl₂.

By varying the wavelength between 330 nm – 900 nm, the OD is measured for each wavelength and the respective wavelength of maximum OD is considered to be λ_{max} for the dye solutions. Observed λ_{max} for Reactive Blue 52 is 615 nm and 406 nm for RO 107, which is matched with the reported values. Solutions of the dyes were standardized by measuring the optical density of the various concentrations of the dye solutions at respective λ_{max}.

Adsorption study

The required quantity of PANI-CoCl₂ and dye in an aqueous medium was taken in 250 ml beaker and placed on a magnetic stirrer which stirred the aliquot at 450 rpm. At regular intervals of time 10 ml of aliquot was withdrawn, centrifuged and filtered. The filtrate was collected separately in a clear dry cuvette and then the optical density of the clear supernatant dye solution was measured and repeated until the equilibrium was attained. The same experiment was conducted at two different weathering conditions. The equilibrium quantity of dye was measured using the formula.

$$q_e = \frac{(C_o - C_e)\,V}{W} \qquad\qquad \dots (1)$$

$$\%\ \text{Decolourisation} = \frac{(C_o - C_t)}{C_o} X\ 100 \qquad \dots (2)$$

Where, C_o (mg/L) and C_t (mg/L) are the initial and final concentration of dye at different time interval t (min.), respectively. q_e (mg/g) is the quantity of dye adsorbed per unit mass of the adsorbent at equilibrium and W (g) is the amount of adsorbent used.

Study on the effect of change of various parameters

Effect of contact time was studied by taking 0.5 g/L of PANI-CoCl₂ with RB 52 (75 mg/L) and 0.4 g/L of PANI-CoCl₂ for RO 107 (90 mg/L). Various sets of experiments were conducted to study the effect of initial dye concentration (55 to 95 mg/L for RB 52 and 50 to 130 mg/L for RO 107), the dose of the adsorbent (0.1to 0.9 g/L), the variation of temperature (30 °C, 40 °C, and 50 °C), alteration of pH of the solution (4 5.84/5.97 and 9) and change in agitation speed (250 to 650 rpm). Desorption experiments were conducted using NaOH and HCl to ascertain the nature of binding of dye molecules onto the composite surface. After adsorption PANI-CoCl₂ composite was filtered, washed with water and then stirred in a magnetic stirrer for 15 min in water, again filtered, dried and required amount of desorbed

adsorbent was taken for adsorption study in successive cycles.

Electrical conductivity

Change in electrical conductivity of PANI-CoCl$_2$ composites was measured using Four Probe set up. The electrical conductivity was measured for PANI-CoCl$_2$ after adsorption of dye by making a pellet of the filtered and dried composite. The same procedure was carried for PANI-CoCl$_2$ before the adsorption of dye.

Results and Discussion

Effect of contact time and comparison by exposing to sunlight

The contact time required to reach equilibrium is an important parameter in the wastewater treatment. The adsorption of dyes on PANI-CoCl$_2$ was studied at a stirring speed of 450 rpm as a function of contact time to determine the equilibrium time. It is found that at 110 min both the dyes attain equilibrium and the percentage of removal is 85% for RB 52 and 89% for RO 107, whereas 100% of decolourisation is possible at lower concentration of dyes. Fig. 3 shows the time of the adsorption equilibrium of RB 52 and RO 107 onto PANI-CoCl$_2$. The removal of dyes was rapid in the initial stages of contact time and gradually decreased with a lapse of time until the equilibrium. The rapid adsorption observed during initial timing is probably due to the abundant availability of active sites on the PANI-CoCl$_2$ surface, and with the gradual occupancy of these sites, the rate of adsorption becomes less[18]. The same experiment was repeated by exposing the reaction aliquot with undoped PANI (PANI-ES) as adsorbent. PANI-CoCl$_2$ has higher adsorption efficiency than PANI-ES. The adsorption study was performed by exposing the reaction system

to direct sunlight (winter at 29 °C and in summer at 34 °C) without stirring using PANI-CoCl$_2$ as adsorbent. More than 75% of RB 52 and RO 107 were removed within 100 min by simple exposure to sunlight, whereas dyes were not decolourised in absence of adsorbent at all the conditions. It was found that the percentage of adsorption increases with an increase in temperature and the variation is depicted in Fig. 4a and 4b for RB 52 and RO 107, respectively.

Effect of initial dye concentration on rate of adsorption

The effect of the change in the initial concentration of dyes using the constant weight of PANI-CoCl$_2$ is shown in Fig. 5. The rate of percentage of adsorption decreases with an increase in the initial concentration of dye which reveals that there is a demand for more active sites for the accommodation of a higher amount of adsorbate. Higher initial dye concentration leads to the saturated occupancy of the active site on the adsorbent surface which leaves unadsorbed dye ion in
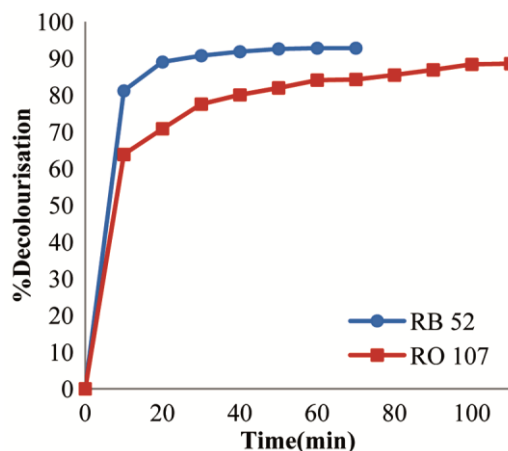

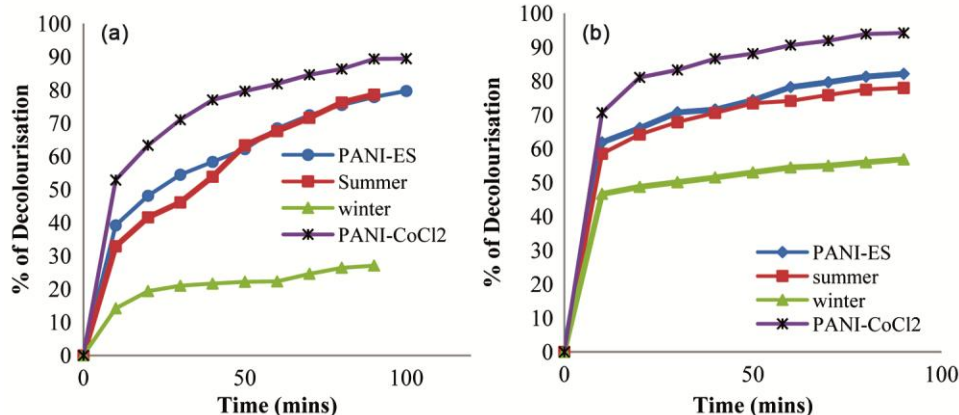Fig. 3 — Plot for effect of contact time for RB 52 and RO 107 adsorption.

Fig. 4 — Plot for comparison of contact time for (a) RB 52 and (b) RO 107 adsorption.

the medium. On the other hand, a lower quantity of dye molecule gets fully adsorbed in a short period of time[19].

Variation of adsorbent concentration

It is observed that the rate of decolourisation increases with an increase in adsorbent dosage upto a certain weight and the plot becomes plateau as shown in Fig. 6. The reason for this increase in removal rate is an increase in the number of surface active sites of PANI-CoCl₂, whereas higher surface active sites will not impart much effect for the dye of same concentration after a saturated dose of adsorbent[20].

Effect of pH

The pH of aliquot will alter the adsorption rate of dyes as shown in Fig. 7. The maximum adsorption was observed at acidic pH and the minimum adsorption was observed at basic pH. In acidic pH electrostatic repulsion between the negatively charged dye anion (Reactive Orange 107 and Reactive Blue 52) and the surface of the adsorbent is lowered, consequently, adsorption efficiency is increased whereas lower adsorption percentage of dye on composite at alkaline condition is probably due to the presence of OH⁻ ion in the solution which is competing with anionic dyes (RB 52 and RO 107) for adsorbent sites[21] and as a result the percentage of decolourisation is decreased with an increase of pH for both the dyes.

Effect of temperature

The adsorption process was carried out at three different temperatures of 30, 40, and 50 °C to verify the effect of temperature by adjusting the temperature controller of the magnetic stirrer. The removal of RB 52 and RO 107 was increased with an increase in the temperature of solution from 30 to 50°C (Fig. 8), which indicates that the adsorption process is endothermic. At higher temperature, acquisition of
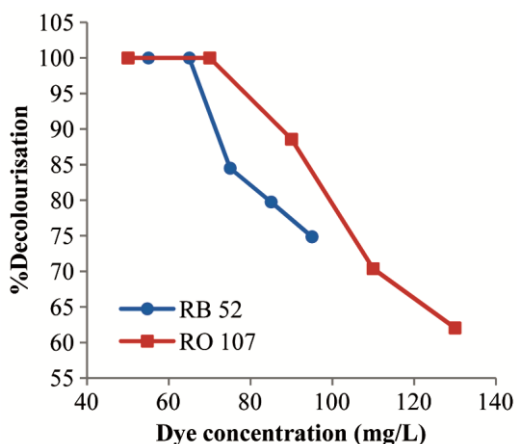
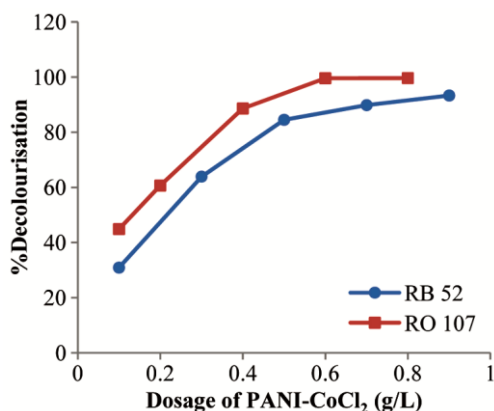Fig. 5 — Plot for effect of initial dye concentration for RB 52 and RO 107 adsorption.

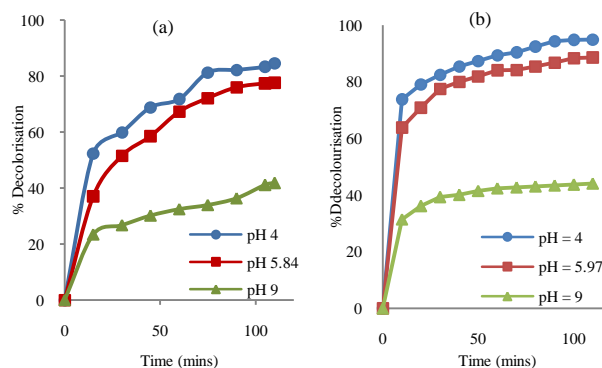Fig. 7 — Plot for effect of pH for (a) RB 52 and (b) RO 107 adsorption.

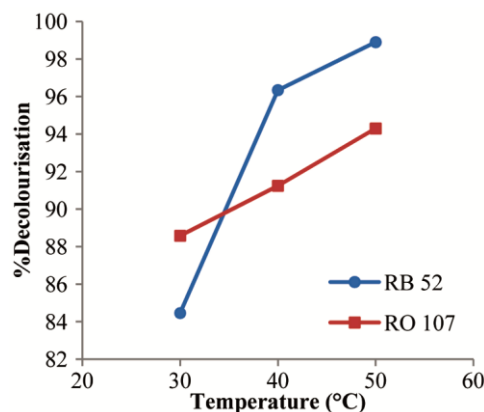Fig. 6 — Plot for effect of dosage of adsorbent for RB 52 and RO 107 adsorption.

Fig. 8 — Plot for effect of temperature for RB 52 and RO 107 adsorption.

sufficient energy as well as higher movement of the dye molecule leads to an easy contact with the active sites of PANI-CoCl$_2$[22].

Effect of agitation speed

Fig. 9 shows the effect of stirring speed (i.e., 250-650 rpm) on the adsorption of RB 52 and RO 107 dyes at constant dye concentrations and adsorbent dosage. The enhancement in adsorbent rate with an increase in stirring speed probably is due to the augmented molecular collision[23]. Therefore, the optimum stirring speed was taken as 450 rpm for the distribution of dye molecule on the surface of the adsorbent.

Desorption studies

After confirming the fact that PANI-CoCl$_2$ is capable of adsorbing the dye molecules onto its surface, it becomes necessary to know the process by which the dye molecules remain adhere to the surface of the composite. In this study desorption experiments were conducted using 0.5 N NaOH, 0.1 N NaOH, 0.025 N NaOH, 0.1 N HCl and 0.025 N HCl to ascertain the nature of binding of dye molecules onto the composite surface. Desorption is shown to have a positive impact on the alkaline medium[24] (Fig. 10) while desorption does not exist in acidic medium. Desorbed adsorbent was used for recyclability. The percentage of dye adsorbed is gradually decreases in the successive cycles[25] as pictured in Fig. 11.

Adsorption isotherm studies

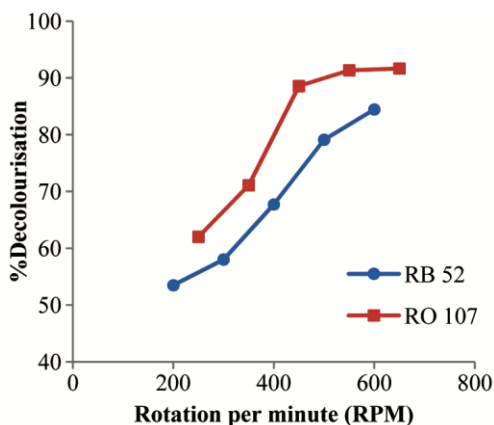An adsorption isotherm explains the relationship between the amount of adsorbate uptaken by the adsorbent and the adsorbate concentration remained in the solution. Adsorption isotherms are essential to understand the nature of the interaction between the adsorbate and the adsorbent used for the removal of pollutants. Although several isotherm equations have been practiced, three important models, Langmuir, Freundlich and Temkin isotherms, were applied in this study.

The Langmuir isotherm is based on the assumption that the adsorption process takes place at specific homogeneous sites within the adsorbent surface and that once a dye molecule occupies a site, no further adsorption can take place at that site. This concluded that the adsorption process is monolayer in nature. The model is represented in linear form as follows.

$$\frac{C_e}{q_e} = \frac{(1+bC_e)}{Q_0 b} \qquad \qquad \ldots (3)$$

Here Q_0 & b are Langmuir constants related to maximum monolayer coverage capacity and b is the constant related to the free energy of adsorption[26]. The plots are shown in Fig. 12. The Freundlich
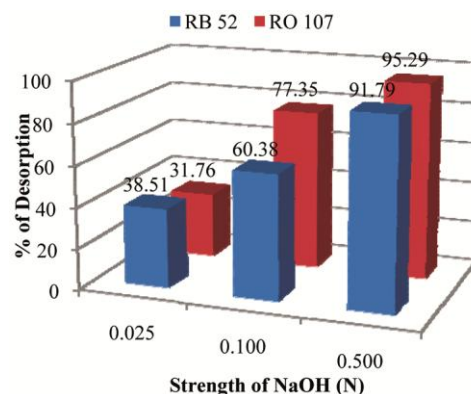
Fig. 10 — Plot for the desorption studies for RB 52 and RO 107 dyes.

Fig. 9 — Plot for effect of agitation speed for RB 52 and RO 107 adsorption.
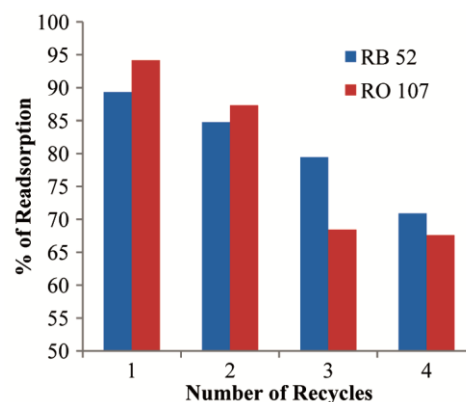
Fig. 11 — Plot for recyclability studies for RB 52 and RO 107 dyes.

isotherm, derived by assuming a heterogeneous surface with a non-uniform distribution of adsorption process over the surface, is presented in the linear form as follows,

$$\ln q_e = \ln K_f + \frac{1}{n}\ln C_e \qquad \dots (4)$$

where K_F is the constant related to the adsorption capacity, and n is the empirical parameter related to the intensity of adsorption. The value of n varies with the heterogeneity of the adsorbent and for favourable adsorption process, the value of it should be less than 10 and higher than unity. Fig. 13 depicts the
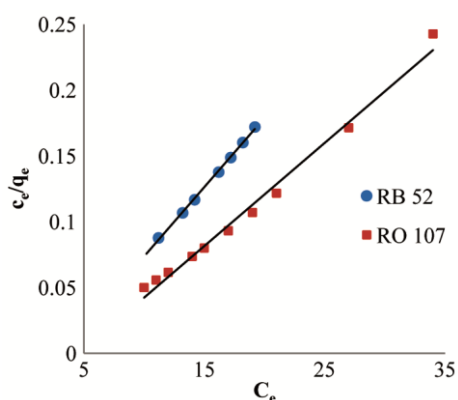

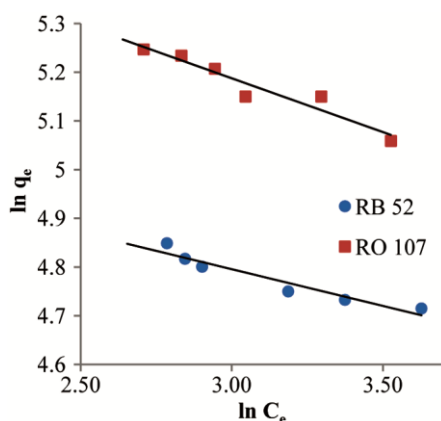Fig. 12 — Graph of Langmuir adsorption isotherm for RB 52 and RO 107 dyes

Fig. 13 — Graph of Freundlich Adsorption Isotherm for RB 52 and RO 107

Freundlich isotherm model. The values of 1/n imply the type of adsorption and can be classified as irreversible (1/n = 0), favorable (0 < 1/n < 1) and unfavorable (1/n > 1) [27]. The obtained values of 1/n are 0.239 for RB 52 and 0.279 for RO 107 showed the favorable nature of both investigated dyes. Temkin isotherm contains a factor that explicitly taking into the account of adsorbent – adsorbate interactions. The derivation of uniform distribution of binding energies was carried out by plotting the quantity adsorbed (q_e) against $\ln C_e$ (Fig. 14). The constants B_T and C were determined from the slope and intercept values, B_T is the variation of adsorption energy related to the heat of adsorption and C is equilibrium binding constant related to the maximum binding energy (L/mg). Table 1 summarizes the different isotherm model constants and their respective correlation coefficients.

Adsorption kinetics

The adsorption rate is an important parameter used to image the adsorption process. Many applications, such as waste water treatment and dye removal need a rapid adsorption rate and short contact time. To investigate the removal of RB 52 and RO 107 using the PANI-CoCl₂ pseudo-second-order equation kinetic model is used. The pseudo-second-order kinetic is usually associated with the rate of adsorption which controls the overall adsorption process. The linear form of the equation is,
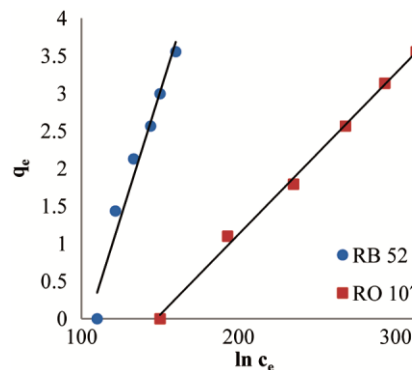
Fig. 14 — Graph of Temkin Adsorption Isotherm for RB 52 and RO 107 dyes.

Table 1 — Different isotherm model constants and their respective correlation coefficients		
Isotherms	R² value	Calculated values
Freundlich	RB52 0.922	RB52 *1/n*=0.239 ; K_F = 228 (L/g)
	RO 107 0.923	RO 107 *1/n*=0.279 ; K_F = 401 (L/g)
Langmuir	RB52 0.998	RB52 Q_0 = 100 mg/g; *b*= 0.35(L/mg); R_L =0.03
	RO 107 0.987	RO 107 Q_0 = 142 mg/g ; *b*= 0.19 L/mg; R_L = 0.05
Temkin	RB52 0.987	RB52 B_T=23.68; A_T =71.53
	RO 107 0.912	RO 107 B_T= 47.09; A_T = 768.70

$$\frac{t}{q_t} = \frac{1}{k_2 q_e^2} + \frac{1}{q_e} t \qquad \qquad \dots (5)$$

The linear plot of (t/q$_t$) against time confirms that the studied adorption process follows pseudo-second-order kinetics. From the plots (Fig. 15), K$_2$, the rate constant are determined (K$_2$ = 7.08x 10^{-4} g/mg/min for RB 52 and K$_2$ = 15.3x10^{-4} g/mg/min for RO 107).

Intraparticle diffusion

The expression for intraparticle diffusion rate constant can be given as

$$q = K_p T^{1/2} + C \qquad \qquad \dots (6)$$

The rate constant for intraparticle diffusion K$_p$ was calculated from the slope of the linear plot of q Vs T$^{1/2}$. The value of K$_p$ calculated for RB 52 is 0.702 and 0.749 for RO 107. From the plot, it was found that the initial sharp portion with subsequent linearity indicated that more than one mode of sorption mechanisms was in operation. The first sharp portion may be due to the instantaneous adsorption of dyes by the external surface of the adsorbent[21]. The next gradual linear portion may be due to the slow intraparticle diffusion stage and it is well observed in Fig. 16.

Thermodynamic parameters

Temperature strongly affects the adsorption of RB 52 and RO 107 on PANI-CoCl$_2$ composite. The adsorption capacity increases with an increase in temperature which comply the endothermic nature of the adsorption reaction. From the data and the following equations, some thermodynamic parameters are calculated. The Gibb's free energy equation is as follows,

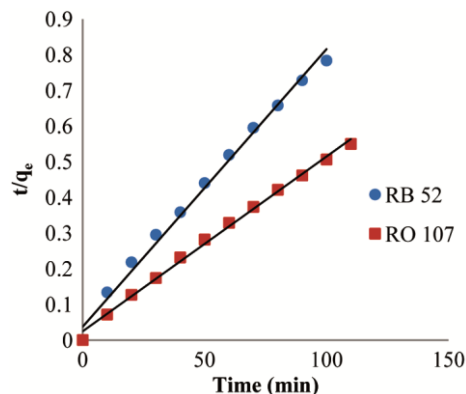$$\Delta G° = -RT \ln K_L \qquad \qquad \dots (7)$$

Fig. 15 — Plot for pseudo second order model for RB 52 and RO 107 dyes.

where K$_L$ is the thermodynamic equilibrium constant that expresses the ratio of dye concentration and PANI-CoCl$_2$ during the adsorption process. The $\Delta G°$ values calculated for different temperatures are negative for both the dyes which indicate that the reaction is spontaneous and feasible under the experimental condition[28] (Table 2).

A graph was plotted for temperature versus lnK$_d$, the slope and the intercept give $\Delta S°$ and $\Delta H°$, respectively. $\Delta H°$ (0.11 kJ mol^{-1} for RO 107 and 0.01 kJ mol^{-1} for RB 52) and $\Delta S°$ (-0.03 J mol^{-1} K^{-1} for RO 107 and -0.027 kJ mol^{-1} for RB 52) are found to correlate with the experimental data. $\Delta H°$ value is positive which indicates that the process is endothermic and $\Delta S°$ is negative which indicates that a decrease in disorderliness, due to adsorption at the interface of PANI-CoCl$_2$ with the dye solution.

ANOVA for correlation coefficients

To analyze the suitability of the three isotherm models and their fitness to the experimental data was assessed. The fitness of the data was established using the coefficients of each isotherm. The isotherms with their R^2 values are shown in Table 3.
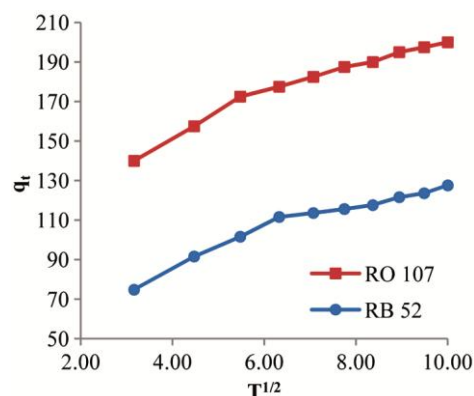
Fig. 16 — Plot for intra particle diffusion for RB 52 and RO 107 dyes.

Table 2 — Calculated $\Delta G°$ values of RB 52 and RO 107

T (°C)	T (K)	$\Delta G°$ for RB 52	$\Delta G°$ for RO 107
30°	303	-9.0069	-8.3736
40°	313	-9.3042	-8.6499
50°	323	-9.6014	-8.9263

Table 3 — Three isotherms with their R^2 values

Isotherms	RB 52	RO 107
Freundlich	0.975	0.917
Langmuir	0.995	0.991
Temkin	0.987	0.912

LINGESWARI & VIMALA: KINETICS, ISOTHERMS AND THERMODYNAMIC MODELLING OF DYES
FROM AQUEOUS SOLUTION USING PANI-CoCl$_2$ AS ADSORBENT

911

In Table 4 ANOVA factor and the summary of the analysis are given. Consideration of the comparative average of the R^2 values and by seeing the variance Langmuir isotherm have least variance which suggests that Langmuir adsorption isotherms model provides a better model for the adsorption of dye molecules onto PANI- CoCl$_2$.

Characterization

SEM Analysis

Scanning Electron Microscopy is widely used to study the morphological features and surface characteristics of the adsorbent materials. The PANI-CoCl$_2$ composite is analyzed by SEM before and after adsorption of RB 52 and RO 107. The PANI-CoCl$_2$ has heterogeneous surface, micro-pores and mesopores as seen from its surface micrographs. In this case, the sponge-like structure with some bright spots confirms the presence of polymer. The flake structure after adsorption may be the dye coverage on PANI-CoCl$_2$ composites as shown in Fig. 17.

FTIR characterization

The FTIR spectrum of prepared PANI-CoCl$_2$ shows all the major bands of PANI-CoCl$_2$. The bands observed at 3436 cm^{-1} were due to secondary N-H stretching vibration. The peak present at 1563 cm^{-1} is attributed to C=N stretching vibration. The C-N stretching vibration of aromatic secondary amine is observed at 1300 cm^{-1}. The peak at 1474 cm^{-1} is attributed to C=C stretching vibration of aromatic compounds. C-H out of plane bending vibration of 1,4 di-substituted aromatic compounds is observed at 801 cm^{-1}. Dye adsorbed PANI-CoCl$_2$ gives different FTIR spectrum compared with unadsorbed PANI-CoCl$_2$ composite as shown in Fig. 18.

Electrical conductivity

It is well known that cobalt doped PANI-CoCl$_2$ composites are semiconductors. The σ values are calculated by using the equation

$$\ln \sigma = \left[\frac{V}{I} \times \frac{\pi}{\ln 2} \times t \right]^{-1} \qquad \dots (8)$$

Where I is the current applied in amperes, V is the voltage measured in volts and t is the thickness in mm. The samples were pressed into a pellet. The temperature dependence of the conductivity of PANI-CoCl$_2$ was measured in the temperature range of 310 to 410 K. The electrical conductivity was measured for the sample made by compaction of PANI-CoCl$_2$ powder. The conductivity of dye adsorbed PANI-CoCl$_2$ is found to be lesser than the PANI- CoCl$_2$ at all temperatures as shown in Fig. 19.

Comparison of effectiveness of PANI-CoCl$_2$ as adsorbent

A detailed review of PANI-based dye adsorption materials is listed in Table 5 to compare maximum

Table 5 — Comparison of the maximum adsorption capacities
of PANI based adsorbents and some dyes

Materials used as Adsorbents	Dye	Maximum Adsorption Capacity(mg/g)	Refrence
PANI-HCl/TMP nanocomposite	MG	78.9	29
PANI-H$_2$SO$_4$	MO	75.9	30
PANI-phytic acid hydrogel	MB	71.2	31
PANI-CSA/polyamide 6 composite	MO	81.9	32
Nanostructured crosslinked PANI	MB	13.8	33
Bioadsorbent	RO 107	28.74	34
Shrimpshell- magnetic nanoparticle	RO 107	95.23	35
PANI-CoCl$_2$	RB 52	100	This study
PANI-CoCl$_2$	RO 107	142	This study

Table 4 — Summary of ANOVA Factors

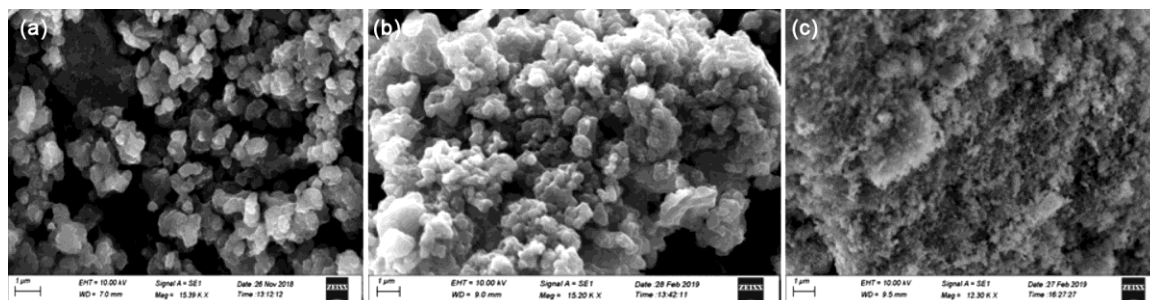| Groups	Count	Sum	Average	Variance
Freundlich	2	1.972	0.986	7.2E-05
Langmuir	2	1.986	0.993	7.2E-05
Temkin	2	1.934	0.967	0.000018

Fig. 17 — SEM images of PANI-CoCl$_2$, (a) before adsorption of any dye, (b) after adsorption of RB 52 dye and (c) after adsorption of RO 107 dye.
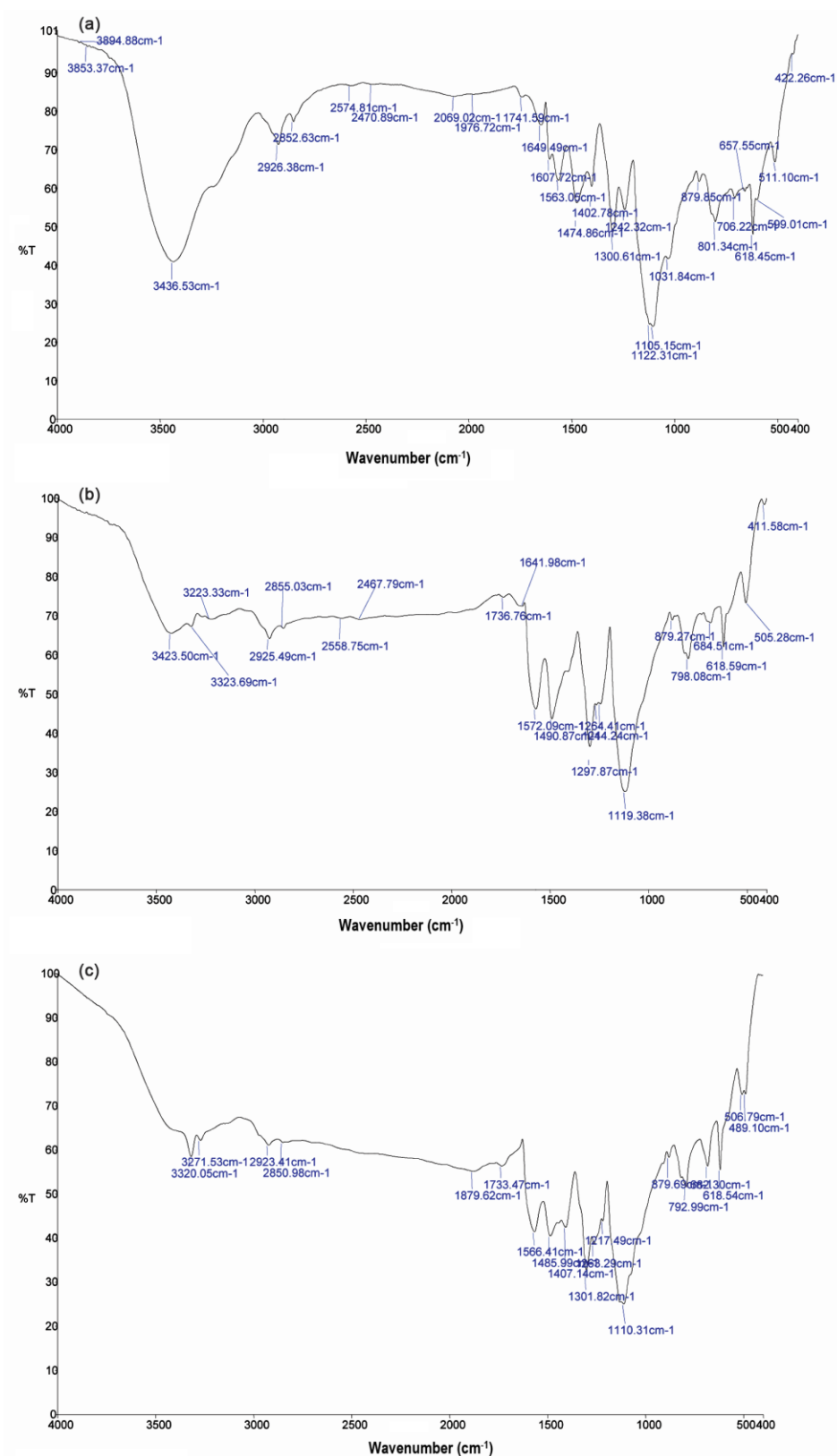
Fig. 18 — FTIR spectra of PANI-CoCl$_2$ (a) before adsorption of any dye, (b) after adsorption of RB 52 dye and (c) after adsorption of RO 107 dye.

LINGESWARI & VIMALA: KINETICS, ISOTHERMS AND THERMODYNAMIC MODELLING OF DYES
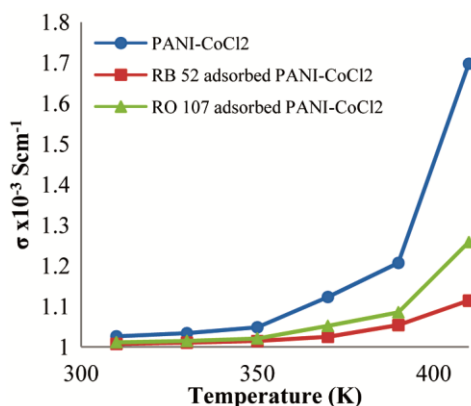FROM AQUEOUS SOLUTION USING PANI-CoCl₂ AS ADSORBENT

913

Fig. 19 — Electrical conductivity plots for PANI-CoCl₂ before and adsorption of RB 52 and RO 107 dyes.

adsorption efficiency with PANI-CoCl₂ as well as the adsorption of RB 52 and RO 107 by other adsorbents.

Conclusions

In this work, the adsorption of Reactive Blue 52 and Reactive Orange 107 onto PANI-CoCl₂ was studied. The modification of PANI salt by doping CoCl₂ increases the adsorption capacity of both the dyes. Three adsorption isotherm models were used to correlate the adsorption experimental data, and it was found that the Langmuir isotherm model gave consistent and reasonable values of fitted parameters. q_e values derived from the kinetic study and experimentally determined amounts of dye adsorbed by the adsorbent at equilibrium are closely related for both dyes. The controlling mechanism of the adsorption of both the dyes onto PANI-CoCl₂ follows electrostatic interaction. Thermodynamic calculations for both dyes indicated that the adsorption was spontaneous.

Reference

1   Manzini B M, Motolese A, Conti A, Ferdani G & Seidenari S, *Contact Dermatitis*, 34(3) (2012) 172.
2   Maureen E Miller, Zana Lummus L & David Bernstein I, *Allergy & Asthma Proc*, 17(1) (1996) 31.
3   Katheresan V, Kansedo J & Lau S Y, *J Environ Chem Eng,* 6(4) (2018) 4676.
4   Zhu M X , Lee L , Wang H H & Wang Z , *J Hazard Mater*, 149(3) (2007) 735.
5   Bhatia D, Sharma N R, Singh J & Kanwar R, *Crit. Rev. Env. Sci. Tec.,* 47 (19) (2017).
6   Tan I A W, Ahmad A L & Hameed B H, *J Hazard Mater*, 154 (2008) 1.
7   Kula I, Uğurlu M, Karaoğlu H & Celik A, *Bioresour Technol*, 99(3) (2008) 492.
8   Namasivayam C, Muniasamy N, Gayatri K, Rani M & Ranganathan K, *Bioresour Technol*, 57(1) (1996) 37.
9   Namasivayam C, Prabha D & Kumutha M, *Bioresour Technol*, 64(1) (1998) 77.
10   Malik P K, *Dyes and Pigments*, 56(3) (2003) 239.
11   Wu F C, Tseng R L & Juang R S, *Environ Technol*, 22(2) (2001) 205.
12   Mahanta D, Madras G, Radhakrishnan S & Patil S J, *Phys Chem B,* 112 (2008) 10153.
13   Chowdhury A N, Jesmeen S R & Hossain M M, *Polym Adv Technol*, 15 (2004) 633.
14   Bingöl D, Veli S, Zor S & Özdemir U, *Synth Met*, 162 (2012) 1566.
15   Vimala T & Anusha D, *Asian J Chem*, 30(1) (2018) 39.
16   Majhi M, Choudhary R B, Thakur A K, Omar F S, Duraisamy N, Ramesh K & Ramesh S, *Polym Bull*, 75(4) (2017) 1563.
17   Majhi M, Choudhary R B & Maji P, *Bull Mater Sci*, 38(5) (2015) 1195.
18   Mehmet Dogan, Hamdi Karaoglu M & Mahir Alkan, *J. Hazard Mater,* 165 (2009) 1142.
19   Ghaedi M, Sadeghian B, Pebdani A, Amiri Sahraei R, Daneshfar A & Duran C, *Chem Eng J*, 187 (2012) 133.
20   Chen D & Ray AK, *Water Res,* 32(11) (1998) 3223.
21   Erol Alver & Aysegül Metin, *Chem Eng J,* 200 (2012) 59.
22   Ahmad M A & Rahman N K, *Chem Eng J,* 170 (2011) 154.
23   Alkan M & Dogan M, *Environ. Bull*, 12 (5) (2003) 418.
24   Jaina R, Gupta V K & Sikarwar S, *J Hazard Mater,* 182 (2010) 749.
25   Baruah P & Mahanta D, *Bull. Mater. Sci,* 39 (2016) 875.
26   Langmuir, *J Am Chem Soc*, 38 (1916) 2221.
27   Greluk M & Hubicki Z, *Chem Eng J,* 162 (2010) 919.
28   Wang L , Zhang Z , Zhao R, Li C, Li Y & Zhang C L, *Desalination,* 254 (2010) 68.
29   Gupta V K, Pathania D, Kothiyal N C & Sharma G, *J Mol Liq*, 190 (2014) 139.
30   Tanzifi M, Hosseini S H, Kiadehi A D, Olazar M, Karimipour K, Rezaiemehr R & Ali I, *J Mol Liq*, 244 (2017) 189.
31   Yan B, Chen Z, Cai L, Chen Z, Fu J & Xu Q, *Appl Surf Sci*, 356 (2015) 39.
32   Xia Y, Li T, Chen J & Cai C, *Synth Met*, 175 (2013) 163.
33   Ayad M & Zaghlol S, *Chem Eng J,* 204 (2012) 79.
34   Ramalakshmi S, Muthuchelian K & Swaminathan K, *J Chem Pharm Res*, 3(6) (2011) 337.
35   Tehreem Saba, Fozia Minhas, Muhammad Imran Malik, Farah Naz Talpur, Abdul Jabbar & Muhammad Iqbal Bhanger, *Am J Analyt Chem*, 9 (2018) 633.